Photophysics of organic semiconductors: from ensemble to the single-molecule level

Rebecca R. Grollman,[a] Whitney E. B. Shepherd,[a] Alexander Robertson,[a] Keshab R. Paudel,[a] John E. Anthony,[b] and Oksana Ostroverkhova[a]

[a]Department of Physics, Oregon State University, Corvallis, OR 97331

[b]Department of Chemistry, University of Kentucky, Lexington, KY 40506

ABSTRACT

We present photophysical properties of functionalized anthradithiophene (ADT) and pentacene (Pn) derivatives, as well as charge and energy transfer properties of donor-acceptor (D/A) pairs of these derivatives. All molecules studied were fluorescent and photostable enough to be imaged on the single-molecule level in a variety of polymeric and in a functionalized benzothiophene (BTBTB) crystalline host using room-temperature wide-field epifluorescence microscopy. Flexibility of functionalization of both guest (ADT, Pn) and host (BTBTB or polymer) molecules can be used for systematic studies of nanoscale morphology and photophysics of D/A organic semiconductor bulk heterojunctions, as well as in applications relying on FRET, using single-molecule fluorescence microscopy.

Keywords: Single molecule fluorescence, organic semiconductors, FRET, charge transfer, photobleaching

1. INTRODUCTION

Organic semiconductors have attracted attention due to their applications in light-emitting diodes, solar cells, thin film transistors, and many others and due to their low cost, easy fabrication, and tunable properties.[1] Most successful organic materials for applications that rely on charge carrier photogeneration (e.g. solar cells) involve donor-acceptor (D/A) bulk heterojunctions (BHJs), properties of which are determined by photoinduced D/A interactions. Examples of these include charge transfer (CT) and Förster resonant energy transfer (FRET), which depend on the photophysical properties of the donor and acceptor molecules, as well as on the nanoscale morphology and local nanoenvironment.[2–8]

Single-molecule fluorescence spectroscopy (SMFS) has been extensively utilized for probing nanoscale interactions and local nanoenviroment in polymers, crystalline solids, and biological systems.[9–11] Single molecules (SM) have also been used as probes of conduction and of exciton dynamics in organic semiconductors.[12–15] However, because of stringent requirements for the good fluorophores for the SMFS (which include high fluorescence quantum yield and high photostability), studies of local nanoenvironment and its effect on photophysics of organic semiconductors have been limited to a handful of materials. In this paper, we discuss high-performance functionalized organic semiconductor materials which are suitable for systematic studies of photophysics which includes charge and energy transfer, both on the macroscopic (device) level and at nanoscales, down to the SM level.

2. EXPERIMENTAL

2.1 Materials and Sample Preparation

In our studies, we used functionalized anthradithiophene (ADT) derivatives with (triethylsilyl)ethynyl (TES) and (triisopropylsilyl)ethynyl (TIPS) side groups (ADT-TES-F and ADT-TIPS-CN, as shown in Fig. 1a) and pentacene (Pn) derivatives with TIPS, NODIPS ((n-octyldiisopropylsilyl)ethynyl), or TCHS ((tricyclohexylsilyl)ethynyl) side groups (Fig. 1b,d) as donors and acceptors for thin-film studies as well as fluorescent guests embedded in a solid host for SMFS. The ADT-TES-F derivative is a high-performance organic semiconductor which exhibits TFT charge carrier mobilities of over 1.5 $cm^2/(Vs)$ in spin-cast films,[16] high photoconductive gains, and fast charge carrier photogeneration.[17,18] Both ADT-TIPS-CN and Pn-R-F8 (R=TIPS, NODIPS, TCHS) derivatives have been used as acceptors in D/A BHJs with polymer or ADT-TES-F donors.[2,4,5,19–21]

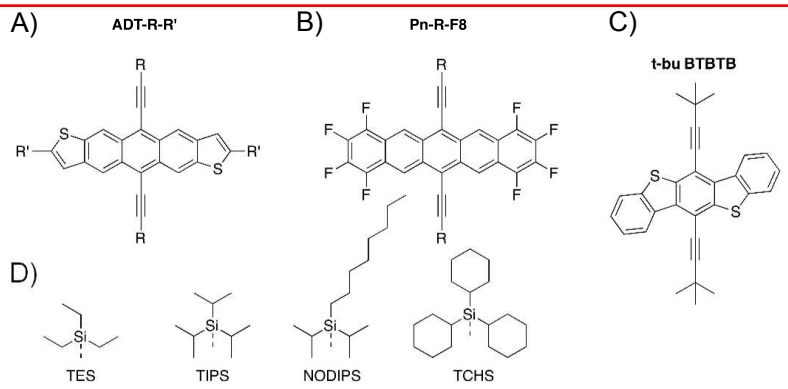

Figure 1. A) ADT-R-R' where R is a side group and R' is an end group (either F or CN), B) Pn-R-F8 where R is a side group, C) t-bu BTBTB, D) Variety of side groups including TES, TIPS, NODIPS, and TCHS.

Pristine films of ADT-R-R' and Pn-R-F8 derivatives exhibit π-stacking,[2] where R-groups control the packing motif.[6]

As host matrices, we chose functionalized benzothiophene derivative t-bu BTBTB (6,12-bis[2-(t-butyl)-ethynyl]benzo[1,2-b:4,5-b']bis(1)benzothiophene, as shown in Fig. 1c), poly(methyl)methacrylate (PMMA), poly-(9-vinylcarbazole) (PVK), and polystyrene (PS). The optical absorption of the t-bu BTBTB derivative, as well as of PMMA, PVK, and PS, is in the UV region,[22] which enables their utility as non-fluorescent hosts for SM imaging at 532 nm and 633 nm. The t-bu BTBTB derivative forms spin-cast polycrystalline films with a dominant (01-1)crystallite orientation[23] and exhibits photoconductivity under UV excitation.[22]

Several types of spin-cast films were prepared. For SMFS, ADT-R-R' or Pn-R-F8 guest molecules were added at 10^{-10} M concentrations to a 1 % wt solution of PMMA (75,000 m.w., Polysciences, Inc.), PVK (1,100,000 m.w., Aldrich), or PS (280,000 m.w., Aldrich) in toluene. Guest molecules at 10^{-12} M concentrations were added to a 10^{-2} M concentration of t-bu BTBTB in tetrahydrofuran (THF). Glass coverslips were soaked in a detergent and water solution overnight. They were then sonicated for 40 minutes in the detergent/water solution, rinsed thoroughly with deionized water, and dried under N_2. After confirming that glass coverslips, solvent, and host matrices were clean in the single-molecule imaging configuration, guest-host samples were spin-cast onto slides for 50 seconds at 3000 rpm for polymer samples and at 2000 rpm for t-bu BTBTB samples.

Spin-cast films for fluorescence lifetime, quantum yield (QY), and photobleaching QY measurements were prepared with higher guest concentrations ("bulk" samples). For QYs, samples were prepared from 10^{-4} M stock solutions of guest molecules in toluene and either 13% wt solution of PMMA in toluene or 10^{-2} M solution of t-bu BTBTB in THF. The concentrations of guest molecules were chosen to achieve the average spacing between guest molecules of 5 to 7 nm, to ensure minimal guest-guest interaction.[24] Spin-cast films for FRET measurements were also prepared with 50/50 mixtures of ADT-TES-F and Pn-F-F8 in PMMA to achieve an average spacing between donor and acceptor molecules of 2 nm. Donor- and acceptor-only samples were also prepared with the same spacing. All "bulk" samples were spin cast at 600 rpm for 50 seconds.

2.2 Photobleaching Quantum Yield

Details of measurements of fluorescence QY and lifetimes have been reported in our previous publications.[2,3,5]

Photobleaching experiments were done with "bulk" samples in the PMMA host under 633 nm (Pn-R-F8) or 532 nm (ADT-R-R') excitation with light intensity (I_λ) of 28 W/cm^2. Similarly, samples in the t-bu BTBTB host were excited with an intensity of 185 W/cm^2. Fluorescence spectra were collected as a function of time with a fiber coupled spectrometer (Ocean Optics USB2000) and integrated over all emission wavelengths for each time frame, ranging from 0.5 to 2 seconds. Most experiments were performed in air, with selected samples measured both in air and in vacuum at 10^{-5} Torr using a micro-cryostat (Janis STC-500) at excitation with light intensity of 0.28 W/cm^2. The photobleaching dynamics of PMMA samples were fit with a bi-exponential ($a_1 exp[-t/\tau_{B1}] + a_2 exp[-t/\tau_{B2}]$) function. The time constant (τ_B) is a weighted average of the two time constants τ_{B1} and

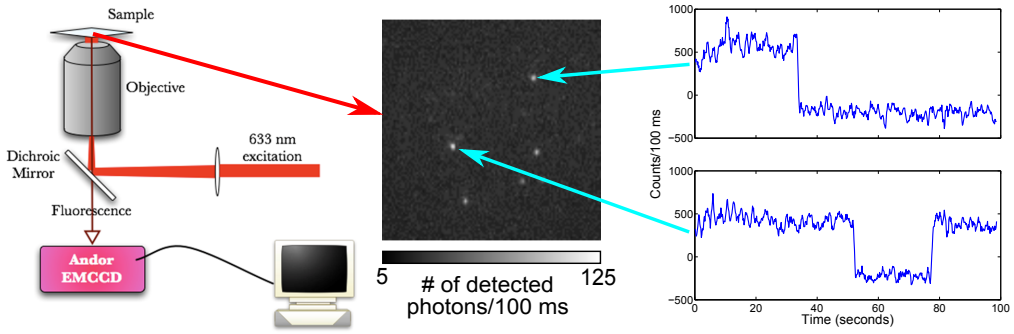

Figure 2. *Left:* Schematic of the experimental set up for single molecule fluorescence spectroscopy. The excitation was 633 nm (532 nm) in the case of Pn-R-F8 (ADT-R-R') derivatives. *Middle:* Image of single molecules of Pn-TCHS-F8 in PMMA. *Right:* Fluorescence time trajectories for the two molecules. The top represents a molecule that photobleaches. The bottom represents a molecule that blinks.

τ_{B2}. The photobleaching dynamics of t-bu BTBTB samples were fit with a single exponential. Photobleaching quantum yield Φ_B was calculated based on Eq. 1

$$\Phi_B = \frac{1}{\tau_B \sigma_\lambda I_\lambda \frac{\lambda}{hc}}, \tag{1}$$

where σ_λ is the absorption cross-section at the wavelength of excitation (λ), h is the Planck constant, and c is the speed of light. The photobleaching quantum yield was also used along with the fluorescence quantum yield (Φ_F) to calculate the total number of photons emitted by the molecule N_{tot} using

$$N_{tot} = \frac{\Phi_F}{\Phi_B}. \tag{2}$$

2.3 Single Molecule Spectroscopy

Single molecule imaging of Pn-R-F8 derivatives and ADT-TIPS-CN was done under circularly polarized 633 nm or 532 nm, respectively, wide-field illumination using an Olympus IX-71 inverted microscope with a 100x UPlanSApo (NA 1.4) oil objective and an Andor iXon EMCCD (DU-897) detector (see Fig. 2). Collection efficiency η_{coll} was determined by $\eta_{coll} = \eta_Q T_{ang} T_{opt} T_{filt}$ where η_Q is the quantum efficiency of the camera (ranging from 85% to 94% depending on the emission from the molecule), T_{ang} is the angular collection factor (34% based on Ha et al.,[25] and Lord et al.[26]), T_{opt} is the collection factor through microscope optics (62% to 68%), and T_{filt} is the transmission through the dichroic and emission filters (21% to 65%).[26] We estimated our collection efficiency to be about 4.6% for ADT-TES-F, 12.0% for ADT-TIPS-CN and 10.6% for Pn-R-F8.

Multiple videos of 600 frames (100 ms/frame) were recorded of each sample in a variety of host matrices. Custom MATLAB scripts then located potential fluorophores and displayed their time trace. Each time trace was reviewed to confirm digital blinking or photobleaching. "On" and "off" counts were calculated based on anything above or below a threshold of three standard deviations above the "off" level, unless stated otherwise. The total number of detected photon N_{tot} was determined again using data collected from the single molecule time traces. The total number of detected photons was calculated by integrating the each time trace (without the background) over it's lifetime. Histograms of the number of detected photons were fit to a single-exponential function ($exp[-N/N_{tot,det}]$) to determine the number of detected photons $N_{tot,det}$. The number of emitted photons $N_{tot,em}$ was calculated by dividing $N_{tot,det}$ by the collection efficiency η_{coll} defined above.

3. RESULTS AND DISCUSSION

Photophysical properties of functionalized ADT and Pn derivatives under study are summarized in Table 1. High fluorescence QYs were observed in toluene; these were further improved when the molecules were incorporated into a solid host. The photobleaching QY, also shown in Table 1, is the probability that a molecule would photobleach upon absorption of a photon. Partial fluorination of the molecular backbone in functionalized ADT, Pn, or hexacene derivatives has been realized as an effective means to improve stability of the molecule against oxidation due to substitution of the most reactive site and electronic structure changes induced by electron-negative fluorine substituent. For example, under the same illumination conditions, in air, Pn-R-F8 molecules dispersed in PMMA were considerably more photostable than their counterparts (Pn-R) with no fluorine substitution (Fig. 3a). The residual photodegradation of ADT-R-R and Pn-R-F8 derivatives dispersed in PMMA observed in air was significantly reduced in vacuum (Fig. 3b), which confirms that photobleaching of these molecules is largely due to photoinduced reaction with oxygen. In PMMA, the values of Φ_B of (1 - 2.5) $\times$ 10^{-6} obtained in ADT and Pn derivatives (Table 1) were comparable with those of commonly used SMFS fluorophores (e.g. dicyanomethylenedihydrofuran (DCDHF) derivatives), in a similar environment.[26,27] The photobleaching QYs for the Pn-R-F8 molecules embedded in the crystalline t-bu BTBTB host were more than an order of magnitude lower than those in PMMA, depending on the derivative, in part due to a reduced oxygen diffusion in the t-bu BTBTB crystalline environment. High fluorescence QYs and high photostability exhibited by ADT-R-R' and Pn-R-F8 derivatives under study enabled their imaging in a variety of hosts (PMMA, PVK, PS, and t-bu BTBTB) at the single molecule level under wide-field excitation at either 532 nm (ADT-R-R') or 633 nm (Pn-R-F8) (Fig.2b). Effects of different host environments on the single-molecule photophysics will be reported elsewhere.[23]

Table 1. Photophysical properties of functionalized organic semiconductors under study.

Molecule	λ_{abs}[a] **(nm)**	λ_{em}[b] **(nm)**	Φ_F[c] **(PMMA)**	τ[d] **(ns)**	Φ_B,[e] 10^{-6}	N_{tot},[f] 10^5 **(bulk)**	$N_{tot,em}$,[g] 10^5 **(SM)**
ADT-TES-F	528	536	0.7 (0.9)	9.4	1.1	8.2	7.7
ADT-TIPS-CN	582	590	0.76 (0.89)	12.7	2.5	3.6	2.4
Pn-TIPS-F8	635	645	0.6 (0.8)	9.4	1.9	4.2	4.7
Pn-NODIPS-F8	635	645	0.53 (0.67)	6.4	1.2	5.6	3.8
Pn-TCHS-F8	637	647	0.61 (0.82)	8.7	1.0	8.2	9.4

[a] Wavelengths of lowest energy absorption maximum measured in dilute toluene solutions.
[b] Wavelengths of maximal emission measured in dilute toluene solutions.
[c] Fluorescence QY in toluene. The values in parenthesis are from bulk samples in PMMA.
[d] Fluorescence lifetime in toluene.
[e] Photobleaching QY of Eq. 1 obtained in bulk samples in PMMA.
[f] Total number of emitted photons calculated using Eq. 2.
[g] Mean number of total emitted photons obtained from single exponential fits to SM histograms.

The total number of photons emitted $N_{tot,em}$ in single molecule studies were similar to those that were calculated through Eq. 2 from photobleaching-related fluorescence decays measured in "bulk" samples (Fig.3). For example, the SM value $N_{tot,em}$ of 2.4×10^5 photons emitted compared well to 3.6×10^5 photons from the "bulk" value for ADT-TIPS-CN in PMMA (Table 1). Nevertheless, we tested the robustness of the approach we used in our MATLAB script that selects fluorophores from the video, analyzes SM fluorescence time trajectories such as those in Fig.2, and calculates $N_{tot,em}$. In particular, we varied the threshold which separates the "on" and "off" states of the molecule (e.g. Pn-TCHS-F8 in PMMA in Fig. 4) and determined the variation in the obtained values of $N_{tot,em}$. For Pn-TCHS-F8 molecules in PMMA, this yielded the range of $N_{tot,em}$ between 6.9×10^5 and 9.4×10^5 photons, which provides an estimate for the analysis-related error in the $N_{tot,em}$ values.

It has been previously shown that ADT-TES-F/ADT-TIPS-CN blends exhibit either FRET (with the FRET

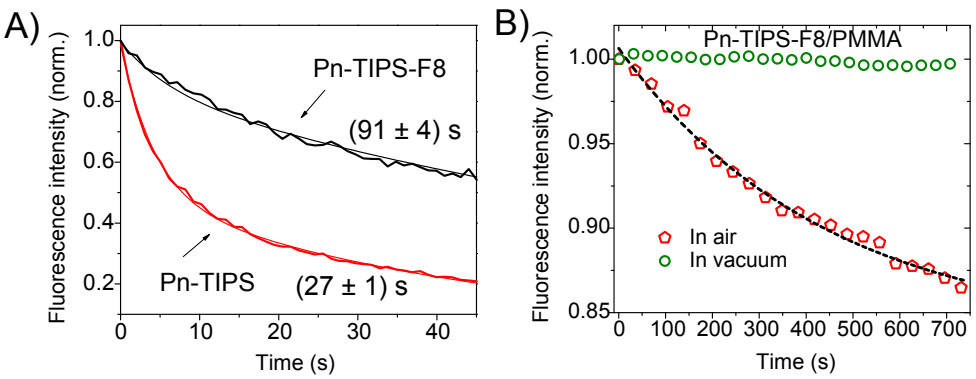

Figure 3. A) Fluorescence decay due to photobleaching under a 633 nm excitation in a non-fluorinated Pn-TIPS vs a fluorinated Pn-TIPS-F8 derivative in PMMA. Bi-exponential fits and the time constants τ_B are also shown. B) Fluorescence decay in air vs vacuum for Pn-TIPS-F8 in PMMA under 633 nm illumination.

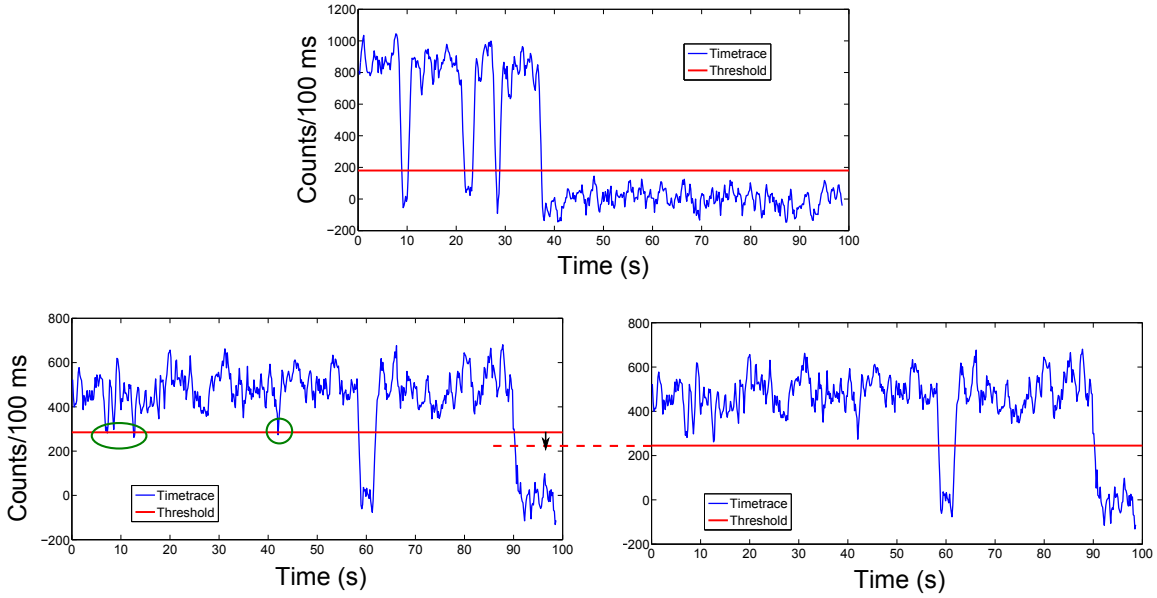

Figure 4. Examples of single-molecule fluorescence time trajectories with various thresholds that separate "on" and "off" states of the molecule. The threshold level was varied to determine how it affects data analysis. Top: Threshold level three standard deviations above the average "off" counts/100 ms. Bottom: Example of threshold that has been lowered such that "on" noise does not interfere with the threshold.

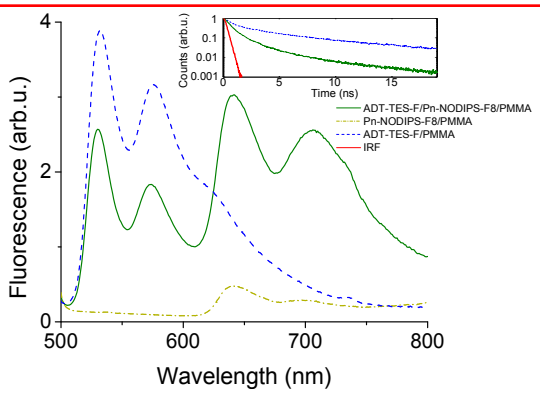

Figure 5. Fluorescence spectra of ADT-TES-F in PMMA (donor-only), Pn-NODIPS-F8 in PMMA (acceptor-only), and ADT-TES-F/Pn-NODIPS-F8 in PMMA (donor/acceptor pair) obtained under 490 nm excitation. FRET from ADT-TES-F to Pn-NODIPS-F8 is observed. Inset shows donor fluorescence lifetime decay obtained under a 532 nm 470 ps pulsed excitation of ADT-TES-F in PMMA (donor-only) samples and in ADT-TES-F/Pn-NODIPS-F8 in PMMA (D/A) samples. The instrument response function (IRF) is also included.

radius of 4.8 nm) or emissive CT state formation (exciplex) with peak emission at ∼669 nm depending on the spacing between the ADT-TES-F donor and ADT-TIPS-CN acceptor molecules.[20] Similar trends were observed in ADT-TES-F/Pn-R-F8 blends, in which the emission efficiency and lifetime of exciplex significantly depended on the size of the acceptor's R-group, so that larger R groups led to a less emissive and shorter lived exciplex.[2,5] If the ADT-TES-F donor and Pn-R-F8 acceptor molecules are separated by a neutral spacer such as PMMA, FRET, with the FRET radius of 4.2-4.5 nm, depending on the side group R, dominates over the exciplex formation. FRET between ADT-TES-F donor and Pn-NODIPS-F8 acceptor molecules is illustrated in Fig.5 which shows fluorescence spectra from ADT-TES-F donor-only, Pn-NODIPS-F8 acceptor-only, and ADT-TES-F/Pn-NODIPS-F8 D/A pair in PMMA under a 490 nm excitation. In the film containing both donor and acceptor molecules, the fluorescence emission from the acceptor was enhanced due to FRET while the the emission from the donor decreased. The ADT-TES-F donor lifetime also decreased due to FRET (inset of Fig. 5). Our ability to image both donor and acceptor molecules on the single molecule level enables studies which rely on the single-molecule FRET, in various hosts and with an additional benefit of donor and acceptor functionalization flexibility.

4. CONCLUSIONS

In summary, we characterized photophysical properties of functionalized anthradithiophene and pentacene derivatives. All molecules studied were imaged on the single-molecule level in polymeric (PMMA, PVK, PS) and crystalline (t-bu BTBTB) hosts using wide-field illumination at room temperature. High fluorescence quantum yields and low photobleaching quantum yields approaching those of standard SMFS fluorophores were obtained. FRET with the FRET radius between 4.2 and 4.8 nm, depending on the acceptor, was observed with the ADT-TES-F as the donor and other ADT and Pn derivatives as acceptors. Our studies lay foundations for systematic studies of local environment on photophysics of organic semiconductors at nanoscales and for applications relying on FRET in these materials using SMFS.

ACKNOWLEDGMENTS

We thank K. Bilty for assistance in imaging of Pn-R-F8 in PVK and PS. This work was supported by the National Science Foundation via CAREER program (DMR-0748671) and grant DMR-1207309.

REFERENCES

1. O. Ostroverkhova, ed., *Handbook of organic materials for optical and (opto)electronic devices*, Woodhead Publishing, Cambridge, U.K., 2013.

2. K. Paudel, B. Johnson, A. Neunzert, M. Thieme, B. Purushothaman, M. M. Payne, J. E. Anthony, and O. Ostroverkhova, "Small-molecule bulk heterojunctions: Distinguishing between effects of energy offsets and molecular packing on optoelectronic properties," *Journal of Physical Chemistry C* **117**, pp. 24752–24760, 2013.
3. A. D. Platt, J. Day, S. Subramanian, J. E. Anthony, and O. Ostroverkhova, "Optical, fluorescent, and (photo)conductive properties of high-performance functionalized pentacene and anthradithiophene derivatives," *Journal of Physical Chemistry C* **113**, pp. 14006–14014, 2009.
4. A. D. Platt, M. J. Kendrick, M. Loth, J. E. Anthony, and O. Ostroverkhova, "Temperature dependence of exciton and charge carrier dynamics in organic thin films," *Physical Review B* **84**, p. 235209, 2011.
5. M. J. Kendrick, A. Neunzert, M. M. Payne, B. Purushothaman, B. D. Rose, J. E. Anthony, M. M. Haley, and O. Ostroverkhova, "Formation of the donor-acceptor charge-transfer exciton and its contribution to charge photogeneration and recombination in small-molecule bulk heterojunctions," *Journal of Physical Chemistry C* **116**, pp. 18108–18116, 2012.
6. J. E. Anthony, "Functionalized acenes and heteroacenes for organic electronics," *Chemical Reviews* **106**, pp. 5028–5048, 2006.
7. O. Ostroverkhova and W. E. Moerner, "Organic photorefractives: Mechanisms, materials and applications," *Chemical Reviews* **104**, pp. 3267–3314, 2004.
8. T. Ameri, P. Khoram, J. Min, and C. J. Brabec, "Organic ternary solar cells: a review," *Advanced Materials* **25**, pp. 4245–4266, 2013.
9. W. E. Moerner, "A dozen years of single-molecule spectroscopy in physics, chemistry, and biophysics," *Journal of Physical Chemistry B* **106**, pp. 910–927, 2002.
10. W. E. Moerner, "New directions in single-molecule imaging and analysis," *Proceedings of the National Academy Sciences USA* **104**, pp. 12596–12602, 2007.
11. W. E. Moerner and M. Orrit, "Illuminating single molecules in condensed matter," *Science* **283**, pp. 1670–1676, 1999.
12. J. M. Lupton, "Single-molecule spectroscopy for plastic electronics: Materials analysis from the bottom-up," *Advanced Materials* **22**, pp. 1689–1721, 2010.
13. B. Kozankiewicz and M. Orrit, "Single-molecule photophysics, from cryogenic to ambient conditions," *Chemical Society Reviews* **43**, pp. 1029–1043, 2014.
14. J. Bolinger, K. J. Lee, R. Palacios, and P. F. Barbara, "Detailed investigation of light induced charge injection into a single conjugated polymer chain," *Journal of Physical Chemistry C* **112**, pp. 18608–18615, 2008.
15. P. F. Barbara, A. J. Gesquiere, S. J. Park, and Y. J. Lee, "Single-molecule spectroscopy of conjugated polymers," *Accounts of Chemical Research* **38**, pp. 602–610, 2005.
16. S. Park, D. A. Mourey, S. Subramanian, J. E. Anthony, and T. N. Jackson, "High-mobility spin-cast organic thin film transistors," *Applied Physics Letters* **93**, p. 043301, 2008.
17. J. Day, A. D. Platt, O. Ostroverkhova, S. Subramanian, and J. Anthony, "Organic semiconductor composites: influence of additives on the transient photocurrent," *Applied Physics Letters* **94**, p. 013306, 2009.
18. J. Day, A. Platt, S. Subramanian, J. Anthony, and O. Ostroverkhova, "Influence of organic semiconductor-metal interfaces on the photoresponse of functionalized anthradithiophene thin films," *Journal of Applied Physics* **105**, p. 103703, 2009.
19. K. R. Rajesh, K. Paudel, B. Johnson, R. Hallani, J. E. Anthony, and O. Ostroverkhova, "Design of organic ternary blends and small-molecule bulk heterojunctions: photophysical considerations," *Journal of Photonics for Energy* **5**, p. 057208, 2015.
20. W. E. B. Shepherd, A. D. Platt, M. J. Kendrick, M. Loth, J. E. Anthony, and O. Ostroverkhova, "Energy transfer and exciplex formation and their impact on exciton and charge carrier dynamics in organic films," *Journal of Physical Chemistry Letters* **2**, pp. 362–366, 2011.
21. K. Paudel, B. Johnson, M. Thieme, M. Haley, M. M. Payne, J. E. Anthony, and O. Ostroverkhova, "Enhanced charge photogeneration promoted by crystallinity in small-molecule donor-acceptor bulk heterojunctions," *Applied Physics Letters* **105**, p. 043301, 2014.

22. W. E. B. Shepherd, A. D. Platt, M. Loth, J. E. Anthony, and O. Ostroverkhova, "Optical, photoluminescent, and photoconductive properties of functionalized anthradithiophene and benzothiophene derivatives," *Proc. of SPIE* **7599**, p. 75990R, 2010.
23. W. E. B. Shepherd, R. Grollman, A. Robertson, K. Paudel, J. E. Anthony, and O. Ostroverkhova, "Single-molecule imaging of organic semiconductors: nanoscale insights into photophysics and molecular packing," submitted 2015.
24. W. E. B. Shepherd, A. D. Platt, D. Hofer, O. Ostroverkhova, M. Loth, and J. E. Anthony, "Aggregate formation and its effect on (opto)electronic properties of guest-host organic semiconductors," *Applied Physics Letters* **97**, p. 163303, 2010.
25. T. J. Ha, T. Laurence, D. S. Chemla, and S. Weiss, "Polarization spectroscopy of single fluorescent molecules," *Journal of Physical Chemistry B* **103**, p. 6839, 1999.
26. S. J. Lord, Z. Lu, H. Wang, K. A. Willets, P. J. Schuck, H. D. Lee, S. Y. Nishimura, R. J. Twieg, and W. E. Moerner, "Photophysical properties of acene dcdhf fluorophores: Long-wavelength single-molecule emitters designed for cellular imaging," *Journal of Physical Chemistry A* **111**, pp. 8934–8941, 2007.
27. K. A. Willets, O. Ostroverkhova, M. He, R. J. Twieg, and W. E. Moerner, "Novel fluorophores for single-molecule imaging," *Journal of the American Chemical Society* **125**, p. 1174, 2003.